Available on CMS information server

CMS DN -2015/009

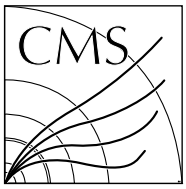

The Compact Muon Solenoid Experiment

Detector Note

The content of this note is intended for CMS internal use and distribution only

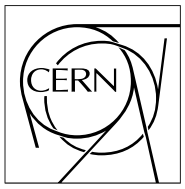

27 February 2015 (v3, 03 July 2015)

Optimizations of light-collection efficiency and uniformity for liquid-scintillator tiles

Zishuo Yang, Young Ho Shin, Sarah Eno, Alberto Belloni, Joshua Samuel

Abstract

Extreme radiation hardness makes liquid-scintillator tile a candidate for future hadron calorimeters. In this note, we present our simulation results of tile light- collection efficiency and uniformity using GEANT4. We point out optimizations that can be made to liquid-scintillator tiles.

The Compact Muon Solenoid Experiment

Detector Note

The content of this note is intended for CMS internal use and distribution only

2015/07/03
Head Id: 278934
Archive Id: 279307M
Archive Date: 2015/02/27
Archive Tag: trunk

Optimizations of light-collection efficiency and uniformity for liquid-scintillator tiles

Zishuo Yang, Young Ho Shin, Sarah Eno, Alberto Belloni, and Joshua Samuel
University of Maryland, College Park

Abstract

Extreme radiation hardness makes liquid-scintillator tile a candidate for future hadron calorimeters. In this note, we present our simulation results of tile light-collection efficiency and uniformity using GEANT4. We point out optimizations that can be made to liquid-scintillator tiles.

Contents

1 Introduction

Future hadron calorimeters require scintillator tiles to withstand significantly high radiation dosage while providing good signal response[1]. Organic liquid-scintillators have extreme radiation hardness (no observable decrease in light yield after 50 Mrad of Co-60 irradiation[2]), which makes liquid-scintillator tile a good candidate for future hadron calorimeters. The University of Maryland is developing and testing prototype tiles with EJ-309 liquid-scintillator from Eljen Technology[1]. To optimize the light-collection efficiency and uniformity, we use GEANT4 Monte Carlo toolkit[3] to simulate optical processes inside a liquid-scintillator tile.

2 Liquid scintillator tile

The prototype tile mainly consists of three parts: an Aluminum container, support tubes, and WLS optical fibers (see Figure 1). The Aluminum container and support tubes together hold the liquid-scintillator inside the tile. Support tubes are made of transparent material such as quartz or sapphire, which with the right refractive index can help to collect optimal amount of light. Wavelength-shifting (WLS) fibers capture photons, shift their wavelengths, and guide them towards a PMT for readout.

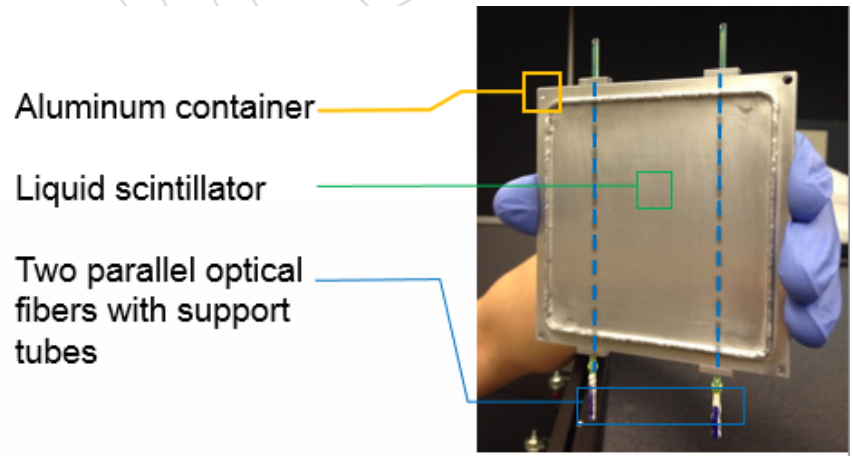

Figure 1: A prototype liquid-scintillator tile with liquid optical fibers.

[1]Eljen Technology, 1300 W. Broadway, Sweetwater, Texas, United States

3 A GEANT4 simulation

The optical GEANT4 simulation includes the following processes:

- refraction;
- reflection;
- wavelength shifting (absorption and re-emission);
- attenuation (non-WLS absorption).

We simulate the $100 \times 100 \times 4\,\mathrm{mm}^3$ tile as shown below (Figure 2).

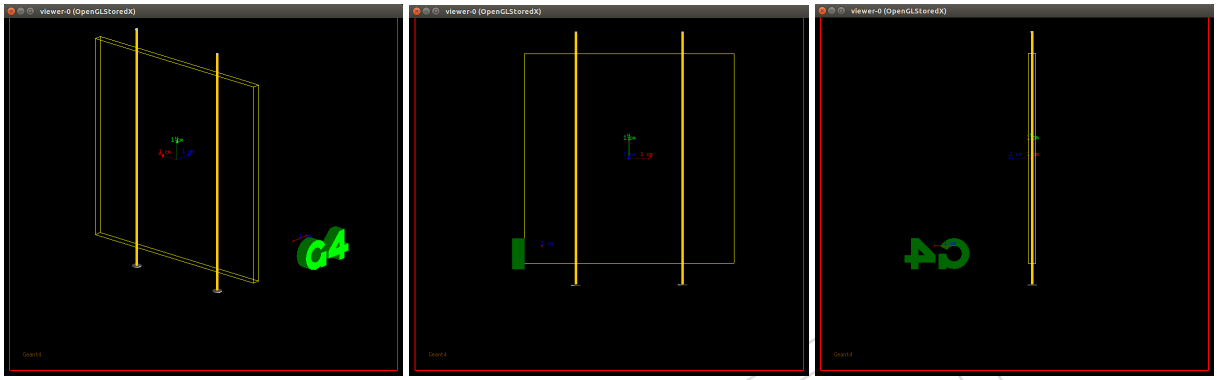

Figure 2: Simulated liquid-scintillator tile in GEANT4.

The Aluminum container in the simulation is a box with reflective inner surface. The reflectivity is an independent parameter, close to typical Aluminum reflectivity (~ 0.9). The optical process at surface boundary is either absorption or reflection, with reflection's probability set by the reflectivity value. The reflection is non-diffusive (or "Specular Spike" in GEANT4 documentation).

The liquid-scintillator in the simulation has density, atomic ratio, refractive index (1.57), and absorption length (2 m) set according to EJ-309 manufacturer's data-sheet [4]. The optical processes include reflection and refraction at scintillator surface boundaries, as well as attenuation inside scintillator.

The support tubes are two parallel tubes through scintillator and container, with absorption length and refractive index close to typical quartz or sapphire. Typical quartz (SiO_2) has a refractive index between 1.46 and 1.55; Typical sapphire (Al_2O_3) has a refractive index of 1.77. The support tube refractive index is a crucial parameter which affects the number of photons getting into optical fibers, and the number of photons escaping optical fibers. The tube outer diameter is constrained by the tile thickness (4 mm); The tube inner diameter is constrained by optical fiber's diameter.

There are three options of fiber-capillary composites in the simulation:

- plastic
- liquid
- liquid w/ additional capillary

For the plastic fiber, an air gap exists between the fiber cladding and support tube inner surface. For the liquid fiber, support tubes hold liquid WLS core inside and keeps liquid-scintillator outside; no air gap exists between WLS core and support tube. For the liquid fiber with addi-

tional capillary, the quartz capillary holds liquid WLS core inside; an air gap exists between the capillary and support tube inner surface. In summary, the overall structure of fiber-capillary composite is as following:

Fiber-capillary composite option	WLS core	Cladding	Air gap	Support tube
Plastic	Yes	Yes	Yes	Yes
Liquid	Yes	No	No	Yes
Liquid w/ additional capillary	Yes	Yes (capillary)	Yes	Yes

On one end of optical fiber, a mirror reflects photons back. On the other end of optical fiber, a perfect PMT registers photons that reach its window (see Figure 3).

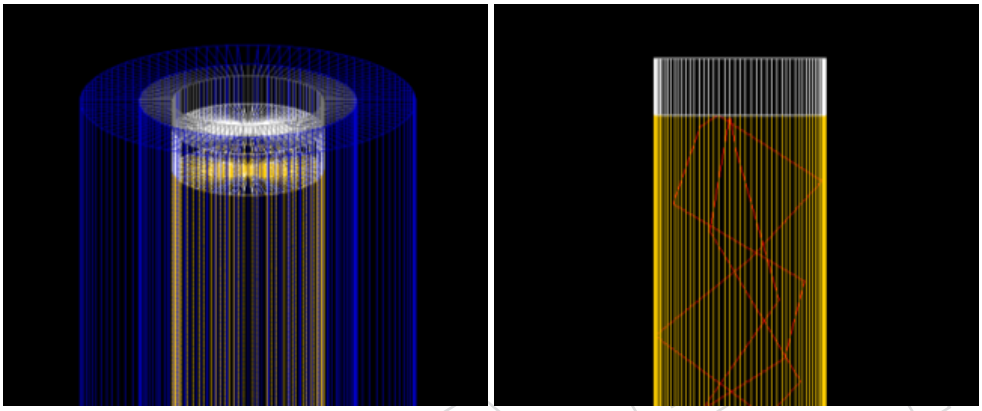

Figure 3: One the left, plastic composite option includes support tube (in blue), air gap (in Gray), and optical fiber (in yellow). On the right, a mirror (in white) on one end of optical fiber reflects photons (in red).

In the simulation, photons with wavelengths corresponding to EJ-309 fluorescence emission spectrum are randomly generated inside the tile (see Figure 4). The majority of photons is killed due to Aluminum reflectivity and EJ-309 attenuation length. The fraction of photons reaching WLS fibers gets absorbed and re-emitted according to WLS core's emission spectrum. The re-emitted photons are assigned with random momentum vectors and linear polarization vectors. A re-emitted photon propagates until it escapes from fiber and gets absorbed, or reaches the PMT window at the end of fiber after multiple reflections. We calculate the light-collection efficiency e,

$$e = \frac{N_{detected}}{N_{generated}} \ , \tag{1}$$

while varying individual construction parameters.

4 Optimization Results

4.1 Aluminum reflectivity

We randomly generate 200,000 photons inside the tile at various reflectivity values. The simulation results show how light-collection efficiency is dependent on reflectivity of Aluminum container. Polishing or mirroring container's inner surface considerably improves light-collection efficiency.

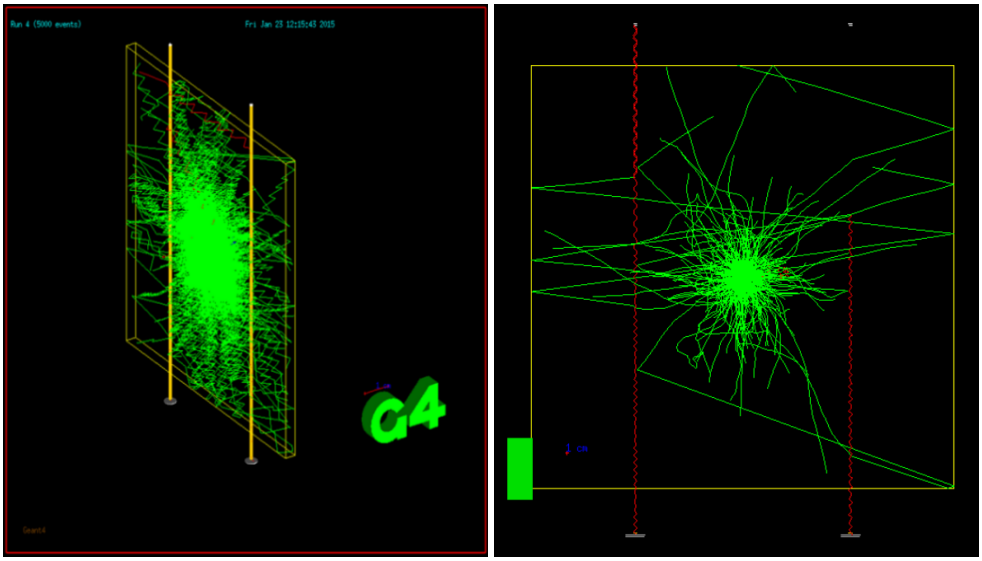

Figure 4: The left figure shows 5000 photons (in green) generated inside liquid-scintillator tile; The right figure shows 2 re-emitted photons (in red) detected by the PMT (gray disks at the bottom).

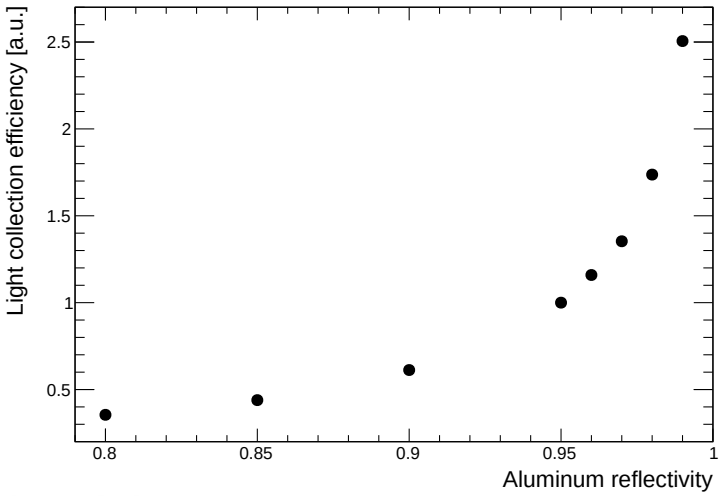

Figure 5: Simulated results of light-collection efficiency vs. Aluminum reflectivity.

4.2 Fiber separation distance

The two parallel fibers are separated by a certain distance, which is constrained tile size. We randomly generate 200,000 photons inside the tile at various fiber separation distances. For the $100 \times 100 \times 4\,\mathrm{mm}^3$ tile, light-collection efficiency is optimized when fiber separation distance is between 30 mm and 70 mm.

4.3 Tile uniformity

Because light-collection efficiency is optimized when fiber separation distance is between 30 mm and 70 mm, we simulate three cases with separation distance equal to 40, 50 and 60 mm. The beam is set to be point-like ($1 \times 1\,\mathrm{mm}^2$), randomly generating 200,000 photons at different

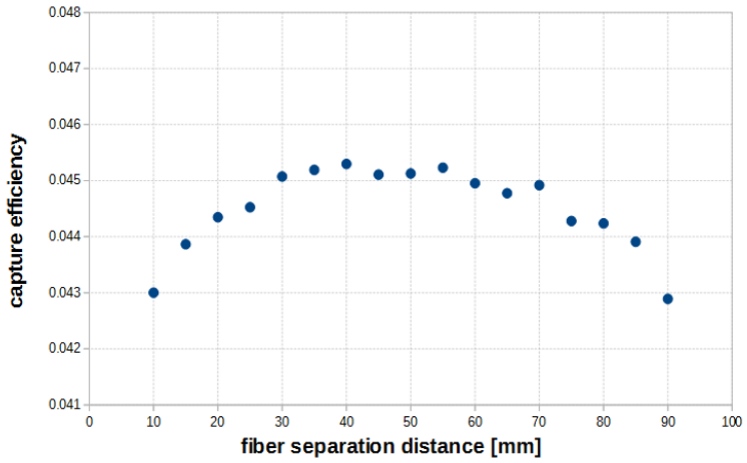

Figure 6: Simulated results of light-collection efficiency vs fiber separation distance.

78 locations across the tile. Effectively, we scan light-collection efficiency in the direction perpendicular to optical fibers.

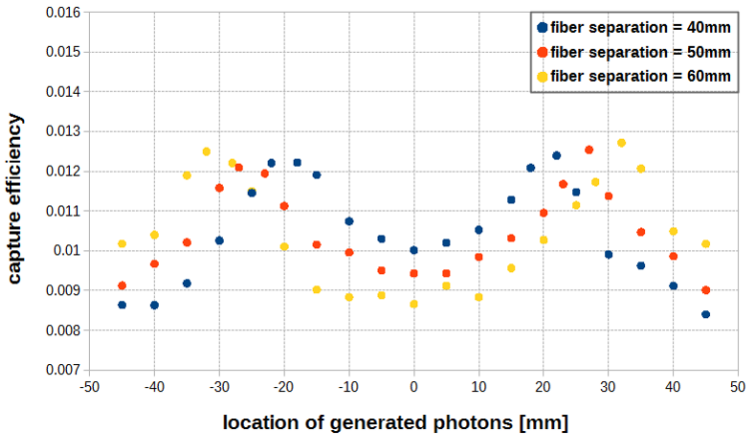

Figure 7: Simulated results of light-collection efficiency vs location of generated photons.

79

80 We calculate the standard deviation of light-collection efficiency in the three cases. The results
81 are shown in table 1.

Fiber separation distance [mm]	mean(μ)	σ/μ
40	0.01050±0.00002	0.1225±0.0002
50	0.01049±0.00002	0.1003±0.0002
60	0.01049±0.00002	0.1280±0.0004

Table 1: Table of signal variances in three cases: 40, 50, and 60 mm fiber separation distance.

82 In the case of $100 \times 100 \times 4\,mm^3$ tile, signal uniformity is optimized when fiber separation
83 distance is close to 50 mm.

4.4 Fiber-capillary composite options

We compare light-collection efficiencies between six fiber-capillary composite options, including:

- plastic + quartz support tube ($n_{refractive}$=1.46);
- plastic + sapphire support tube ($n_{refractive}$=1.77);
- liquid + quartz support tube ($n_{refractive}$=1.46);
- liquid + quartz support tube ($n_{refractive}$=1.55);
- liquid + sapphire support tube ($n_{refractive}$=1.77);
- liquid w/ quartz capillary + quartz support tube ($n_{refractive}$=1.46).

The radiation damage effect on WLS fibers is simulated by decreasing WLS core's absorption length. In the case of plastic WLS core, we roughly estimate absorption length to be 0.01 m after 20 Mrad radiation damage[5]; In the case of liquid WLS core, we keep absorption length unchanged after radiation damage. This is justified by liquid organic scintillator's extreme rad-hardness. For each fiber-capillary composite option, we randomly generate 200,000 photons inside tile. We compare light-collection efficiency before and after radiation damage. Simulation results show that plastic WLS fiber with quartz support tube has high capture efficiency before radiation damage. Replacing quartz with sapphire (higher refractive index) would further improve efficiency, but not significantly. Liquid WLS fiber with lower-refractive-index support tube (quartz $n_{refractive}$=1.46) has high light-collection efficiency. After radiation damage, liquid WLS fiber's light-collection efficiency is significantly higher than plastic WLS fiber.

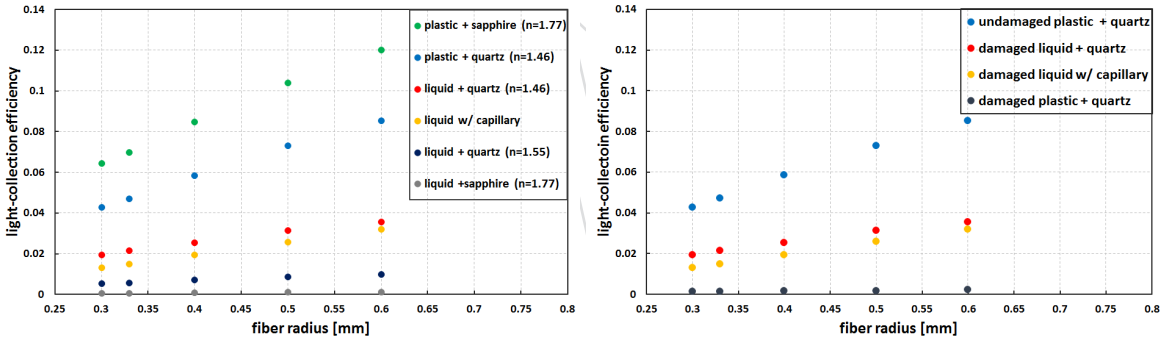

Figure 8: The left figure shows light-collection efficiency vs. fiber radius before radiation damage; The right figure shows light-collection efficiency vs. fiber radius after radiation damage.

5 Conclusions

We use GEANT4 Monte Carlo toolkit to simulate a liquid-scintillator tile prototype. Based on GEANT4 optical-photon-simulation results, we find that the light-collection efficiency can be improved by polishing or mirroring tile's inner surface. $100 \times 100 \times 4\,mm^3$ liquid-scintillator tile's light-collection uniformity and efficiency can be optimized when fiber separation distance is close to 50 mm. We compare various fiber-capillary composite options before and after roughly estimated radiation damage. We find that plastic WLS fibers with high-refractive-index support tube gives high light-collection efficiency, and liquid WLS fibers with low-refractive-index support tube gives high light-collection efficiency. After radiation damage, liquid WLS fiber's light-collection efficiency is significantly higher than plastic WLS fiber.

References

[1] C. Collaboration, "CMS Technical Design Report for the Phase 1 Upgrade of the Hadron Calorimeter", (2012) 14.

[2] A. Belloni et al., "Liquid-scintillator tiles for high-radiation environments", (2015). In preparation.

[3] GEANT4 Collaboration, "GEANT4: A Simulation toolkit", *Nucl.Instrum.Meth.* **A506** (2003) 250–303, doi:10.1016/S0168-9002(03)01368-8.

[4] Eljen Technology, "EJ-309 liquid scintillator pulse-shape discrimination properties", 2010. http://www.eljentechnology.com/index.php/products/liquid-scintillators/73-ej-309. Accessed November-14-2014.

[5] Y. Protopopov and V. Vasil'chenko, "Radiation damage in plastic scintillators and optical fibers", *Nuclear Instruments and Methods in Physics Research Section B: Beam Interactions with Materials and Atoms* **95** (1995), no. 4, 496 – 500, doi:http://dx.doi.org/10.1016/0168-583X(94)00599-0.